High order ENO/WENO methods for conservation laws

Zhengfu Xu

Michigan Technological University

August 1, 2020

Outline

- Review of the general conservation law computation.

Outline

- Review of the general conservation law computation.
- Issues of reconstruction and numerical fluxes.

Outline

- Review of the general conservation law computation.
- Issues of reconstruction and numerical fluxes.
- Bound preserving flux limiters.

Outline

- Review of the general conservation law computation.
- Issues of reconstruction and numerical fluxes.
- Bound preserving flux limiters.
- Provable total variation bounded flux limiters and convexity preserving flux limiters.

Outline

- Review of the general conservation law computation.
- Issues of reconstruction and numerical fluxes.
- Bound preserving flux limiters.
- Provable total variation bounded flux limiters and convexity preserving flux limiters.
- Conclusion and remark.

Entropy solution of nonlinear hyperbolic conservation laws

The well known facts about the entropy solution to

$$u_t + f(u)_x = 0$$

include:

1. There could be contact discontinuity, rarefaction or shock appearing in the solution given well prepared initial data.
2. The solution is piecewise smooth if initial condition is smooth. This provides the theoretical argument for high order approximation.
3. More complex in multi-dimension and hyperbolic system. Interaction between waves, vortex in solution and some extreme situations.

[Joel Smoller, Shock waves and reaction-diffusion equations.]

Challenges for computation

1. The major difficulty is to design a scheme with **both** high accuracy and robustness for computer simulation.
2. There are other tricky matters. To resolve contact discontinuity, a scheme with least diffusion is preferred. However, a certain amount of diffusion is necessary to allow for rarefaction and shock solution.
3. There is almost no theoretical work for solving hyperbolic system even though all the schemes for scalar problems are extended to systems.

Low order VS high order

Advantages of low order methods:

1. Robust and easy to implement, LF, LLF scheme for example.
2. Solid theoretical results: monotone scheme can be proven to produce numerical results convergent to the entropy solution of the scalar conservation laws. [Crandall, M. G., Majda, A., Monotone difference approximations for scalar conservation laws.]

Low order VS high order

Advantages of low order methods:

1. Robust and easy to implement, LF, LLF scheme for example.
2. Solid theoretical results: monotone scheme can be proven to produce numerical results convergent to the entropy solution of the scalar conservation laws. [Crandall, M. G., Majda, A., Monotone difference approximations for scalar conservation laws.]

Advantages of high order methods:

1. High accuracy, therefore less grids to resolve the solution.
2. Low dissipation and better resolution for turbulence simulations. For example, double Mach, Rayleigh-Taylor instability simulation.

Low order VS high order

Advantages of low order methods:

1. Robust and easy to implement, LF, LLF scheme for example.
2. Solid theoretical results: monotone scheme can be proven to produce numerical results convergent to the entropy solution of the scalar conservation laws. [Crandall, M. G., Majda, A., Monotone difference approximations for scalar conservation laws.]

Advantages of high order methods:

1. High accuracy, therefore less grids to resolve the solution.
2. Low dissipation and better resolution for turbulence simulations. For example, double Mach, Rayleigh-Taylor instability simulation.

One's advantage exposes the other's disadvantage. Most of the recent work focuses on improving efficiency and stability of ENO/WENO methods.

Key Words

Main concepts for discussion while solving

$$u_t + f(u)_x = 0$$

numerically:

1. High order accuracy: High order polynomial reconstruction.
2. Stability: bound preserving; total variation bounded.
3. Conservation: the scheme can be written as

$$u_j^{n+1} = u_j^n - \lambda(\hat{f}_{j+\frac{1}{2}} - \hat{f}_{j-\frac{1}{2}}),$$

   therefore the conservation $\sum_j u_j^{n+1} = \sum_j u_j^n$. Here $\lambda = \frac{\Delta t}{\Delta x}$.

The framework of finite volume method

Finite volume (FV) formulation: integrate $u_t + f(u)_x = 0$ over $[x_{j-\frac{1}{2}}, x_{j+\frac{1}{2}}]$

$$\frac{d\bar{u}_j}{dt} = -\frac{f(u(x_{j+1/2},t)) - f(u(x_{j-1/2},t))}{\Delta x} \tag{1}$$

evolving $\bar{u}_j = \frac{1}{\Delta x}\int_{I_j} u dx$. With numerical fluxes introduced, we are staring at

$$\frac{d\bar{u}_j}{dt} = -\frac{\hat{f}(u^-_{j+\frac{1}{2}}, u^+_{j+\frac{1}{2}}) - \hat{f}(u^-_{j-\frac{1}{2}}, u^+_{j-\frac{1}{2}})}{\Delta x} \tag{2}$$

1. $\bar{u}_j \rightarrow u^{\pm}_{j+1/2}$ by some polynomial reconstruction becomes necessary. For example, for a first order finite volume method, we can simply let $u^-_{j+\frac{1}{2}} = \bar{u}_j, u^+_{j+\frac{1}{2}} = \bar{u}_{j+1}$.
2. The introduction of approximate numerical fluxes again is for stability consideration, formally drawn from approximate Riemann solver. As another key component of a numerical scheme, the numerical flux is generally needed to be consistent and Lipschitz continuous wrt all the inputs.

Polynomial reconstructions.

Notations

For the uniform partition

$$a = x_{\frac{1}{2}} < x_{\frac{3}{2}} < \cdots < x_{N+\frac{1}{2}} = b,$$

with a spacing Δx, denote the subinterval $I_j := [x_{j-1/2}, x_{j+1/2}]$ and its center $x_j := \frac{1}{2}(x_{j-1/2} + x_{j+1/2})$.

The process of polynomial reconstructions is to find some $p(x) \in \mathcal{P}^{k-1}(I_j)$ for each cell I_j such that it gives a k-th order accurate approximation to some given function $v(x)$ inside I_j. Precisely speaking,

$$\bar{v}_j := \frac{1}{\Delta x} \int_{x_j-1/2}^{x_j+1/2} v(x)dx \equiv \frac{1}{\Delta x} \int_{x_j-1/2}^{x_j+1/2} p(x)dx. \tag{3}$$

Linear reconstructions

Ignoring boundary conditions while assuming $\bar{v}_j$ is available for $j \leq 0$ and $i > N$ if needed.

A polynomial $p(x) \in \mathcal{P}^{k-1}(I_j)$ can be uniquely constructed over the stencil

$$S(j) := \{I_{j-r}, I_{j-r+1}, \cdots, I_{j+s}\}, \text{ where } r+1+s=k, \tag{4}$$

by interpolating on cell averages $\{\bar{v}_{j-r}, \bar{v}_{j-r+1}, \cdots, \bar{v}_{j+s}\}$. For example, for a 3rd order approximation on the right cell boundary of I_j

$$\hat{v}^-_{j+\frac{1}{2}} = \sum_{i=0}^{k-1} c_{ri}\bar{v}_{j-r+i}, \tag{5}$$

we have three choices of the stencil, the coefficients c_{ri} are shown in the Table 1:

Table 1: The coefficients c_{ri} in (5)

k	r	i =0	i =1	i =2
1	-1	1		
	0	1		
2	-1	3/2	-1/2	
	0	1/2	1/2	
	1	-1/2	3/2	
3	-1	11/6	-7/6	1/3
	0	1/3	5/6	-1/6
	1	-1/6	5/6	1/3
	2	1/3	-7/6	11/6

[Shu, ICASE report]

linear reconstructions across discontinuity

When the given data $\bar{u}_j$ is obtained from a smooth function, the linear reconstruction performs well. However, when discontinuity exists, oscillation appears in the reconstruction (Gibbs phenomenon). As a result, the approximation property

$$p(x) = v(x) - \mathcal{O}(\Delta x^k)$$

is no longer valid.

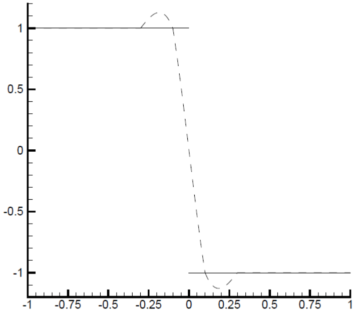

Figure 1: Solid: a step function. Dashed: fixed central stencil cubic interpolation approximation.

ENO reconstructions

A smart polynomial reconstruction: Essentially Non-Oscillatary (ENO [1], [2], [3]) by adaptively choosing the stencil $S(j)$ for **each** I_j to avoid including the discontinuous cell to $S(j)$ if possible. So here is the question: Why the word "essentially"?

[1] [Harten, Osher, Engquist, and Chakravarthy, 1986]
[2] [Harten & Osher, 1987]
[3] [Harten, Engquist, Osher, and Chakravarthy, 1987]

To achieve this, we look at the primitive of the original function $v(x)$, i.e.

$$V(x) := \int_{-\infty}^{x} v(s)ds. \tag{6}$$

Clearly, the divided differences over grid points $\{\cdots, x_{j-\frac{1}{2}}, x_{j+\frac{1}{2}}, \cdots\}$,

$$\begin{aligned} V[x_{j-\frac{1}{2}}] &:= V(x_{j-\frac{1}{2}}), \\ V[x_{j-\frac{1}{2}}, \cdots, x_{j+i-\frac{1}{2}}] &:= \frac{V[x_{j+\frac{1}{2}}, \cdots, x_{j+i-\frac{1}{2}}] - V[x_{j-\frac{1}{2}}, \cdots, x_{j+i-\frac{3}{2}}]}{x_{j+i-\frac{1}{2}} - x_{j-\frac{1}{2}}}. \end{aligned} \tag{7}$$

Remark: It could be easily verified that

$$\begin{aligned} V[I_j] &:= V[x_{j-\frac{1}{2}}, x_{j-\frac{1}{2}}] = \bar{v}_j \\ V[I_{j-1}, I_j] &:= V[x_{j-\frac{3}{2}}, x_{j-\frac{1}{2}}, x_{j+\frac{1}{2}}] = \frac{\bar{v}_j - \bar{v}_{j-1}}{2\Delta x} \\ V[I_j, I_{j+1}] &:= V[x_{j-\frac{1}{2}}, x_{j+\frac{1}{2}}, x_{j+\frac{3}{2}}] = \frac{\bar{v}_{j+1} - \bar{v}_j}{2\Delta x} \\ &\cdots\cdots \end{aligned} \tag{8}$$

ENO Procedure

For each cell $I_j = [x_{j-\frac{1}{2}}, x_{j+\frac{1}{2}}]$, start with the 1-cell stencil $S_1(j) := \{I_j\}$.

1. Compute the divided differences over the two candidate stencils
$$S_{2L}(j) := \{I_{j-1}, I_j\}, \quad S_{2R}(j) := \{I_j, I_{j+1}\},$$
that is to evaluate the values $V[I_{j-1}, I_j]$ and $V[I_j, I_{j+1}]$.

   Determine the 2-cell stencil by
$$S_2(j) := \begin{cases} S_{2L}(j), & \left|V[I_{j-1}, I_j]\right| < \left|V[I_j, I_{j+1}]\right| \\ S_{2R}(j), & \left|V[I_{j-1}, I_j]\right| \geq \left|V[I_j, I_{j+1}]\right| \end{cases}$$
2. Based on $S_2(j)$, do a similar process in step 1 to get $S_3(j)$, $\cdots$, until the desired order of accuracy is achieved, i.e. the k-cell stencil $S_k(j)$.
3. Determine the polynimial $p_j(x) \in \mathcal{P}^{k-1}(I_j)$ based on the $S_k(j)$.

One Example

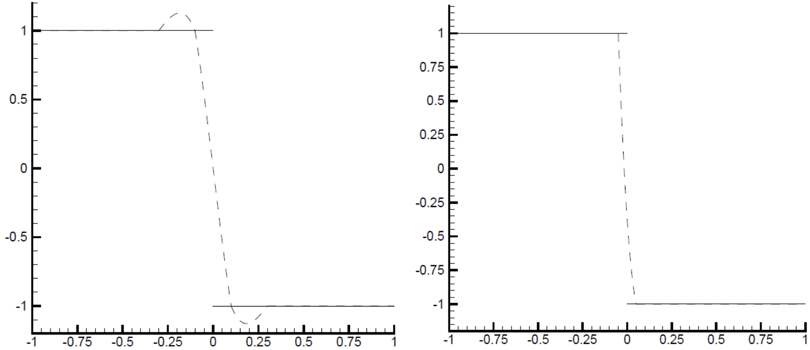

Figure 2: Left: Fixed central stencil cubic interpolation. Right: ENO cubic interpolation. Solid: the same step function. Dashed: interpolant piecewise cubic polynomial approximations.

Remarks on ENO Reconstructions

Remark: The above ENO reconstruction is uniformly high order accurate right up to the discontinuity.

However,

- In the stencil choosing process, for each cell I_j, k candidate stencils are considered, covering $2k-1$ cells. But only one of the stencils is actually used in the final calculations of $p_j(x)$.
  If all $2k-1$ cells in the potential stencils are used, one could get $(2k-1)$-th order of accuracy in smooth regions.
- So, let's introduce WENO.

WENO Reconstructions

Weighted ENO (WENO[4]) is designed by using a convex linear combination of all k-cell stencils (or equivalently to say, using the information from all $2k-1$ cells, $\{I_{j+s}\}_{s=-(k-1)}^{s=k-1}$).

[4] [Liu, Osher, Chan, 1994]

WENO Reconstructions

Weighted ENO (WENO[4]) is designed by using a convex linear combination of all k-cell stencils (or equivalently to say, using the information from all $2k-1$ cells, $\{I_{j+s}\}_{s=-(k-1)}^{s=k-1}$).

Precisely, given fixed stencil reconstruction $v(x_{j+\frac{1}{2}})$ as

$$v_{j+\frac{1}{2}}^{(r)} := \sum_{i=0}^{k-1} c_{ri}\,\bar{v}_{j-r+i}, \quad r = 0, 1, \cdots, k-1. \tag{9}$$

WENO reconstruction takes

$$\hat{v}_{j+\frac{1}{2}} := \sum_{r=0}^{k-1} \omega_r\, v_{j+\frac{1}{2}}^{(r)} \tag{10}$$

where the weights $\omega_r \geq 0$ and $\omega_0 + \omega_1 + \cdots + \omega_{k-1} = 1$. Clearly, the key to the success of WENO would be the choice of those weights $\{\omega_r\}_{r=0}^{k-1}$ so that the order of accuracy and emulation of ENO near a discontinuity is achieved.

[4] [Liu, Osher, Chan, 1994]

WENO procedure

In 1996, Jiang & Shu considered: for $r = 0, 1, \cdots, k-1$,

$$\omega_r := \frac{\alpha_r}{\alpha_0 + \alpha_1 + \cdots + \alpha_r}, \quad \alpha_r := \frac{d_r}{(\varepsilon + \beta_r)^2}, \tag{11}$$

where d_r is defined as the coefficients in

$$\sum_{r=0}^{k-1} d_r v_{j+\frac{1}{2}}^{(r)} \equiv v(x_{j+\frac{1}{2}}) - \mathcal{O}(\Delta x^{2k-1}),$$

when for a smooth function $v(x)$, the so-called "smooth indicators"

$$\beta_r := \sum_{l=1}^{k-1} \int_{x_{j-\frac{1}{2}}}^{x_{j+\frac{1}{2}}} \Delta x^{2l-1} \left(\frac{\partial^l p_r(x)}{\partial x^l} \right)^2 dx \geq 0,$$

and $p_r(x) \in \mathcal{P}^{k-1}(I_j)$ is the polynomial interpolated on the stencil $S_r(j)$ and the constant $\varepsilon = 10^{-6}$ is to avoid $\beta_r = 0$.

For $k = 2$, we have $d_0 = \frac{2}{3},\ d_1 = \frac{1}{3}$ and

$$\begin{cases} \beta_0 = (\bar{v}_{j+1} - \bar{v}_j)^2, \\ \beta_1 = (\bar{v}_j - \bar{v}_{j-1})^2. \end{cases} \tag{12}$$

For $k = 3$, we have $d_0 = \frac{3}{10},\ d_1 = \frac{6}{10},\ d_2 = \frac{1}{10}$ and

$$\begin{cases} \beta_0 = \frac{13}{12}(\bar{v}_j - 2\bar{v}_{j+1} + \bar{v}_{j+2})^2 + \frac{1}{4}(3\bar{v}_j - 4\bar{v}_{j+1} + \bar{v}_{j+2})^2, \\ \beta_1 = \frac{13}{12}(\bar{v}_{j-1} - 2\bar{v}_j + \bar{v}_{j+1})^2 + \frac{1}{4}(\bar{v}_{j-1} - \bar{v}_{j+1})^2, \\ \beta_2 = \frac{13}{12}(\bar{v}_{j-2} - 2\bar{v}_{j-1} + \bar{v}_j)^2 + \frac{1}{4}(3\bar{v}_{j-2} - 4\bar{v}_{j-1} + \bar{v}_j)^2. \end{cases} \tag{13}$$

......

It can be easily verified that the accuracy condition is satisfied, even near smooth extrema[5]. Nowadays, there are also many other WENO methods[6].

[5] Jiang & Shu, 1996

[6] Ketcheson, Gottlieb, and MacDonald, 2011

Review of conservative high order methods.

High order finite volume method

The semi-discrete form of finite volume method reads as

$$\frac{d\bar{u}_j}{dt} = -\frac{\hat{f}(u^-_{j+\frac{1}{2}}, u^+_{j+\frac{1}{2}}) - \hat{f}(u^-_{j-\frac{1}{2}}, u^+_{j-\frac{1}{2}})}{\Delta x}. \tag{14}$$

With the help of the previously discussed reconstruction, semi-discrete high order finite volume methods are completed by some polynomial reconstruction. For example, find the polynomial $p(x)$ of degree 2 such that

$$\bar{u}_k = \frac{1}{\Delta x}\int_{I_k} p(x)dx, k = j-1, j, j+1.$$

Then let $u_{j+1/2} \approx p(x_{j+1/2})$. Of course, this is a fixed stencil reconstruction. Or we can use ENO/WENO to improve our reconstruction.

High order finite difference method

1. Finite difference (FD) formulation with a sliding function

$$\frac{1}{\Delta x}\int_{x-\frac{\Delta x}{2}}^{x+\frac{\Delta x}{2}} h(\xi)d\xi = f(u(x,t)),$$

$$f(u)_x = \frac{1}{\Delta x}\left(h(x+\frac{\Delta x}{2}) - h(x-\frac{\Delta x}{2})\right),$$

$$\frac{du_j}{dt} = -\frac{1}{\Delta x}\left(h_{j+/2} - h_{j-1/2}\right).$$

2. Treat $f(u)$ as the average volume of some function h, then back to the finite volume reconstruction: $f(u_j) \rightarrow h^-_{j+1/2}$ and $h^+_{j-1/2}$.
3. Reconstructions: Linear; ENO; WENO; or others.

Brief summary

1. We can achieve high order approximation in terms of obtaining highly accurate interface values through polynomial reconstruction.
2. What about stability, robustness? With right time-stepping method, are we guaranteed reliable numerical solutions?
3. What kind of stability do we expect to achieve for convergence purpose or for the purpose of reassuring ourselves the method is reliable to some extent?

Bound preserving (BP) flux limiters.

BP high order scheme for hyperbolic equation

- One dimensional scalar hyperbolic problem

$$u_t + f(u)_x = 0, \quad u(x,0) = u_0(x), \tag{15}$$

with boundary condition. Its entropy solution satisfies:

$$u_m \le u(x,t) \le u_M$$

$$\text{if } u_m = \min_x u_0(x) \text{ and } u_M = \max_x u_0(x)$$

BP high order scheme for hyperbolic equation

- One dimensional scalar hyperbolic problem

$$u_t + f(u)_x = 0, \quad u(x,0) = u_0(x), \tag{15}$$

with boundary condition. Its entropy solution satisfies:

$$u_m \le u(x,t) \le u_M$$

$$\text{if } u_m = \min_x u_0(x) \text{ and } u_M = \max_x u_0(x)$$

- A typical conservative scheme with Euler forward

$$u_j^{n+1} = u_j^n - \lambda(\hat{H}_{j+1/2} - \hat{H}_{j-1/2}), \tag{16}$$

where $\lambda := \frac{\Delta t}{\Delta x}$.

BP high order scheme for hyperbolic equation

- One dimensional scalar hyperbolic problem

$$u_t + f(u)_x = 0, \quad u(x,0) = u_0(x), \tag{15}$$

with boundary condition. Its entropy solution satisfies:

$$u_m \le u(x,t) \le u_M$$

$$\text{if } u_m = \min_x u_0(x) \text{ and } u_M = \max_x u_0(x)$$

- A typical conservative scheme with Euler forward

$$u_j^{n+1} = u_j^n - \lambda(\hat{H}_{j+1/2} - \hat{H}_{j-1/2}), \tag{16}$$

where $\lambda := \frac{\Delta t}{\Delta x}$.

- Numerical solution is bound preserving if:

$$u_m \le u_j^n \le u_M, \text{ for all } j, n$$

Parametrized flux limiters

Looking for limiters of the type

$$\tilde{H}_{j+1/2} = \theta_{j+1/2}(\hat{H}_{j+1/2} - \hat{h}_{j+1/2}) + \hat{h}_{j+1/2} \tag{17}$$

such that the modified numerical scheme satisfies

$$u_m \leq u_j^n - \lambda(\tilde{H}_{j+1/2} - \tilde{H}_{j-1/2}) \leq u_M. \tag{18}$$

$\hat{h}_{j+1/2}$ is the (Satisfy-Everything) first order monotone flux.

Parametrized flux limiters

Looking for limiters of the type

$$\tilde{H}_{j+1/2} = \theta_{j+1/2}(\hat{H}_{j+1/2} - \hat{h}_{j+1/2}) + \hat{h}_{j+1/2} \tag{17}$$

such that the modified numerical scheme satisfies

$$u_m \leq u_j^n - \lambda(\tilde{H}_{j+1/2} - \tilde{H}_{j-1/2}) \leq u_M. \tag{18}$$

$\hat{h}_{j+1/2}$ is the (Satisfy-Everything) first order monotone flux.

- $\theta_{j+1/2} = 0, \quad j = 1, 2, 3, \ldots$: first order scheme with bound-preserving property.

Parametrized flux limiters

Looking for limiters of the type

$$\tilde{H}_{j+1/2} = \theta_{j+1/2}(\hat{H}_{j+1/2} - \hat{h}_{j+1/2}) + \hat{h}_{j+1/2} \tag{17}$$

such that the modified numerical scheme satisfies

$$u_m \leq u_j^n - \lambda(\tilde{H}_{j+1/2} - \tilde{H}_{j-1/2}) \leq u_M. \tag{18}$$

$\hat{h}_{j+1/2}$ is the (Satisfy-Everything) first order monotone flux.

- $\theta_{j+1/2} = 0, \quad j = 1, 2, 3, \ldots$: first order scheme with bound-preserving property.
- $\theta_{j+1/2} = 1, \quad j = 1, 2, 3, \ldots$: high order scheme most likely without bound-preserving property.

Parametrized flux limiters

Looking for limiters of the type

$$\tilde{H}_{j+1/2} = \theta_{j+1/2}(\hat{H}_{j+1/2} - \hat{h}_{j+1/2}) + \hat{h}_{j+1/2} \tag{17}$$

such that the modified numerical scheme satisfies

$$u_m \leq u_j^n - \lambda(\tilde{H}_{j+1/2} - \tilde{H}_{j-1/2}) \leq u_M. \tag{18}$$

$\hat{h}_{j+1/2}$ is the (Satisfy-Everything) first order monotone flux.

- $\theta_{j+1/2} = 0, \quad j = 1, 2, 3, \ldots$: first order scheme with bound-preserving property.
- $\theta_{j+1/2} = 1, \quad j = 1, 2, 3, \ldots$: high order scheme most likely without bound-preserving property.
- $\theta_{j+1/2}$ exists, locally explicitly defined.

[Xu, Math Comp 2014], [Liang & Xu, JSC 2014].

Define $\theta_{j+1/2}$ in general

For each $\theta_{j+1/2}$, we look for upper bounds $\Lambda_-(j)$ and $\Lambda_+(j)$ on I_j. Let

$$\Gamma_j^M := u_M - \left(u_j + \lambda(\hat{h}_{j+1/2} - \hat{h}_{j-1/2})\right) \geq 0,$$
$$\Gamma_j^m := u_m - \left(u_j + \lambda(\hat{h}_{j+1/2} - \hat{h}_{j-1/2})\right) \leq 0,$$

since $\hat{h}_{j+1/2}$ is a first order monotone flux, and denote

$$F_{j\pm1/2} := \hat{H}_{j\pm1/2} - \hat{h}_{j\pm1/2}.$$

To ensure $u_j^{n+1} \in [u_m, u_M]$, it is sufficient to let

$$\theta_{j-1/2}F_{j-1/2} - \theta_{j+1/2}F_{j+1/2} - \frac{1}{\lambda}\Gamma_j^M \leq 0 \tag{19}$$
$$\theta_{j-1/2}F_{j-1/2} - \theta_{j+1/2}F_{j+1/2} - \frac{1}{\lambda}\Gamma_j^m \geq 0 \tag{20}$$

1. To preserve the upper bound in (19), define the pair $\left(\Lambda_{-}^{M}(j), \Lambda_{+}^{M}(j)\right)$,

(a) If $F_{j-\frac{1}{2}} \leq 0$, $F_{j+\frac{1}{2}} \geq 0$,

$$\left(\Lambda_{-}^{M}(j), \Lambda_{+}^{M}(j)\right) = (1, 1).$$

(b) If $F_{j-\frac{1}{2}} \leq 0$, $F_{j+\frac{1}{2}} < 0$,

$$\left(\Lambda_{-}^{M}(j), \Lambda_{+}^{M}(j)\right) = \left(1, \min\left(1, \frac{\Gamma_{j}^{M}}{-\lambda F_{j+1/2}}\right)\right).$$

(c) If $F_{j-\frac{1}{2}} > 0$, $F_{j+\frac{1}{2}} \geq 0$,

$$\left(\Lambda_{-}^{M}(j), \Lambda_{+}^{M}(j)\right) = \left(\min\left(1, \frac{\Gamma_{j}^{M}}{\lambda F_{j-1/2}}\right), 1\right).$$

(d) If $F_{j-\frac{1}{2}} > 0$, $F_{j+\frac{1}{2}} < 0$,

$$\left(\Lambda_{-}^{M}(j), \Lambda_{+}^{M}(j)\right) = \left(\min\left(1, \frac{\Gamma_{j}^{M}}{\lambda F_{j-1/2} - \lambda F_{j+1/2}}\right), \min\left(1, \frac{\Gamma_{j}^{M}}{\lambda F_{j-1/2} - \lambda F_{j+1/2}}\right)\right).$$

2. To preserve the lower bound in (20), define the pair $\left(\Lambda_-^m(j), \Lambda_+^m(j)\right)$,

(a) If $F_{j-\frac{1}{2}} \geq 0,\ F_{j+\frac{1}{2}} \leq 0$,

$$\left(\Lambda_-^m(j), \Lambda_+^m(j)\right) = (1, 1).$$

(b) If $F_{j-\frac{1}{2}} \geq 0,\ F_{j+\frac{1}{2}} > 0$,

$$\left(\Lambda_-^m(j), \Lambda_+^m(j)\right) = \left(1, \min\left(1, \frac{\Gamma_j^m}{-\lambda F_{j+1/2}}\right)\right).$$

(c) If $F_{j-\frac{1}{2}} < 0,\ F_{j+\frac{1}{2}} \leq 0$,

$$\left(\Lambda_-^m(j), \Lambda_+^m(j)\right) = \left(\min\left(1, \frac{\Gamma_j^m}{\lambda F_{j-1/2}}\right), 1\right).$$

(d) If $F_{j-\frac{1}{2}} < 0,\ F_{j+\frac{1}{2}} > 0$,

$$\left(\Lambda_-^m(j), \Lambda_+^m(j)\right) = \left(\min\left(1, \frac{\Gamma_j^m}{\lambda F_{j-1/2} - \lambda F_{j+1/2}}\right), \min\left(1, \frac{\Gamma_j^m}{\lambda F_{j-1/2} - \lambda F_{j+1/2}}\right)\right).$$

Notice that the range of $\theta_{j+1/2} \in [0, 1]$ is required to ensure both the upper and lower bound of the numerical solutions in both cells I_j and I_{j+1}. Thus the locally defined limiting parameter is given by

$$\theta_{j+1/2} := \min\left\{\Lambda_+^M(j),\ \Lambda_-^M(j+1),\ \Lambda_+^m(j),\ \Lambda_-^m(j+1)\right\}. \tag{21}$$

Generalized BP flux limiters:

- A rewriting of third order TVD RK FD WENO scheme:

$$u_j^{n+1} = u_j^n - \lambda(\hat{H}^{rk}_{j+\frac{1}{2}} - \hat{H}^{rk}_{j-\frac{1}{2}}), \tag{22}$$

where

$$\hat{H}^{rk}_{j+\frac{1}{2}} \doteq \frac{1}{6}\hat{H}^{n}_{j+\frac{1}{2}} + \frac{2}{3}\hat{H}^{(2)}_{j+\frac{1}{2}} + \frac{1}{6}\hat{H}^{(1)}_{j+\frac{1}{2}}.$$

- Parametrized BP flux limiters are applied to the final step (the integral form along temporal direction)

$$\tilde{H}^{rk}_{j+\frac{1}{2}} = \theta_{j+\frac{1}{2}}(\hat{H}^{rk}_{j+\frac{1}{2}} - \hat{h}_{j+\frac{1}{2}}) + \hat{h}_{j+\frac{1}{2}} \tag{23}$$

- Applied to incompressible flow problem. [Xiong, Qiu, Xu, JCP 2013]

Comments

- Early work of flux limiters (TVD stability): [J. Boris and D. Book, 1973; S. T. Zalesak, 1979; P. L. Roe, 1982; Van Leer, 1974; R. F. Warming AND R. M. Beam, 1976; P. K. Sweby, 1984]
- The parametrized limiters provide a sufficient condition for high order conservative scheme to be BP.
- The accuracy of the high order scheme with BP limiters will be affected by CFL number.
- Question remains: Does it maintain high order accuracy when applied to FD ENO/WENO?
  In other words, is $\tilde{H}_{j+1/2} - \hat{H}_{j+1/2} = \mathcal{O}(\Delta x^{r+1})$?

Numerical tests: FD3RK3 for $u_t + u_x = 0$

Table 2: $T = 0.5$, $CFL = 0.6$, $u_0(x) = \sin^4(x)$, without limiters.

N	L^1 error	order	L^∞ error	order	$(u_h)_{min}$
20	2.21e-02	–	4.43e-02	–	$-2.26E-02$
40	3.49e-03	2.66	6.48e-03	2.77	$-3.69E-03$
80	4.54e-04	2.94	8.77e-04	2.89	$-5.16E-04$
160	5.76e-05	2.98	1.11e-04	2.98	$-6.68E-05$
320	7.22e-06	3.00	1.40e-05	3.00	$-8.36E-06$

Table 3: $T = 0.5$, $CFL = 0.6$, $u_0(x) = \sin^4(x)$, with limiters.

N	L^1 error	order	L^∞ error	order	$(u_h)_{min}$
20	1.83e-02	–	4.43e-02	–	3.55E-14
40	3.24e-03	2.50	6.48e-03	2.77	1.23E-14
80	4.57e-04	2.82	8.77e-04	2.89	6.38E-23
160	5.75e-05	2.99	1.23e-04	2.83	1.72E-16
320	7.22e-06	2.99	1.71e-05	2.85	9.61E-22

All that can be proven

- FD: For 1-D general nonlinear problem, the general BP flux limiters does not affect the third order accuracy when $\hat{h}$ is local Lax-Friedrich flux.
- FD: When $\hat{h}$ is global Lax-Friedrich flux, BP and third order accuracy are obtained when CFL is less than 0.886.
  [Xiong, Qiu & Xu, JCP, 2013].
- FV: When applied to FV WENO solving general $u_t + f(u)_x = 0$ with LF fluxes (Local or Global), BP and third order accuracy is obtained without extra CFL requirement.

Results and development

BP flux limiters are generalized to convection-dominated diffusion equation [Jiang & Xu, SIAM JSC 2013].

$$\frac{\partial u}{\partial t} + \frac{\partial f(u)}{\partial x} = \frac{\partial^2 A(u)}{\partial x^2}, \tag{24}$$

where $A'(u) \geq 0$. The porous medium equation

$$u_t = (u^m)_{xx}, \quad x \in \mathcal{R}, t > 0, \tag{25}$$

Barenblatt solution

$$B_m(x,t) = t^{-k} \left[\left(1 - \frac{k(m-1)}{2m} \frac{|x|^2}{t^{2k}} \right)_+ \right]^{1/(m-1)}, \tag{26}$$

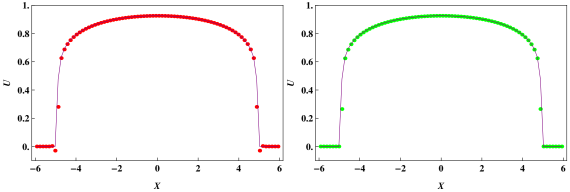

Results and development

Generalized to Euler system for positive density, pressure and internal energy [Xiong, Qiu & Xu, JSC 2016].

High Mach number astrophysical jets: Two high Mach number astrophysical jets without the radiative cooling

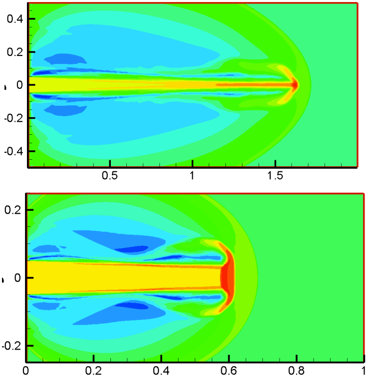

Figure 4: Top: density of Mach 80 at $T = 0.07$; Bottom: density of Mach 2000 at $T = 0.001$

Results and development

Vlasov equation simulation: Ion-acoustic turbulence [Xiong, Qiu & Xu, JCP 2014].

$$\partial_t f_e + v\partial_x f_e - E(t,x)\partial_v f_e = 0, \tag{27}$$

$$\partial_t f_i + v\partial_x f_i + \frac{E(t,x)}{M_r}\partial_v f_i = 0, \tag{28}$$

$$E(t,x) = -\nabla\phi(t,x), \qquad -\Delta\phi(t,x) = \rho(t,x). \tag{29}$$

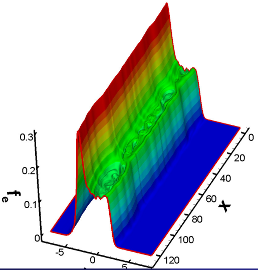

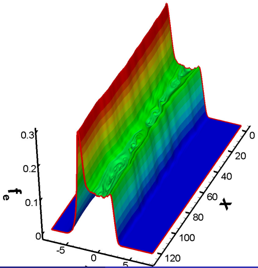

A brief summary

Through modifying the numerical fluxes, we obtained

1. A discrete maximum principle preserving stability.
2. High order accuracy without demanding CFL constraint.
3. Useful application to positivity preserving for compressible Euler simulation and others.

Provable total-variation-bounded (TVB) flux limiters.

Total variation stability for scalar conservation laws

The TV of a real-valued function $g(x)$ on $[a, b]$,

$$TV(g) := \sup_{[x_1, x_2, \dots, x_{p-1}, x_p]} \sum_{j=1}^{p-1} \left| g(x_{j+1}) - g(x_j) \right|,$$

which equals $\int_a^b |g'(x)| dx$ when the function is differentiable.

The entropy solution of $u_t + f(u)_x = 0$ has the contractive & bounded total variation properties:

$$TV(u(\cdot, t_2)) \leq TV(u(\cdot, t_1)) \leq TV(u(\cdot, 0)), \quad \forall t_2 \geq t_1 \geq 0.$$

Bounded variation is critical for investigating existence-uniqueness of solutions to the Cauchy problems, [Bressan].

Discrete total variation stability

1. TV defined by point values:

$$TV_h(u) = \sum_j |u_j - u_{j-1}|,$$

which is not greater than the true total variation

$$TV_h(u) \leq TV(u).$$

2. Classical total variation diminishing (TVD) scheme generally satisfies

$$TV_h(u^{n+1}) \leq TV_h(u^n).$$

thus leads to convergence of the numerical solution to a weak solution of the PDE, [Harten, Glimm].

A sufficient condition for total variation stability: [Harten]

A numerical scheme of the form

$$u_j^{n+1} = u_j^n + C_{j+1/2}^{+}\Delta_{j+1/2}u - C_{j-1/2}^{-}\Delta_{j-1/2}u$$

with $\Delta_{j+1/2}u = u_{j+1}^n - u_j^n$ is TVD if

$$C_{j+1/2}^{\pm} \geq 0 \text{ and } C_{j+1/2}^{+} + C_{j+1/2}^{-} \leq 1.$$

1. Many of the traditional low order schemes satisfy this condition, therefore TVD.
2. The accuracy of the scheme is at most second order.
3. Only first order for two-dimensional problem, [Goodman, Leveque].

Alternatives for high order schemes: TVB stability

$$TV_h(u^{n+1}) \leq (1 + M\Delta t) TV_h(u^n), \qquad (30)$$

i.e. TVB limiters, ENO/WENO schemes, WENO limiters for DG methods.

1. Numerically universal high order accuracy is achieved and oscillation is suppressed.
2. Various issues persist: TVB is not proven; Tuning parameters are needed.

Issues of controlling discrete total variation

1. A universal bound on the updated values u^{n+1} does not necessarily ensure bounded variation. (Local bounds?)
2. The effect of the change of one single function value u_j^{n+1} on the increase of total variation is difficult to characterize. (New measurements?)
3. For general high order methods relying on reconstruction, the total variation of u^{n+1} is not necessarily bounded even if the reconstructed values are exact. (More work on flux limters?)

The question for a bound preserving approach

1. Given $TV_h(u^n) \leq TV(u_0(x))$, can we find some local bounds $u^*_{j,m}, u^*_{j,M}$ in order to achieve
$$TV_h(u^{n+1}) \leq TV(u_0(x))$$
by requiring
$$u^*_{j,m} \leq u^{n+1}_j \leq u^*_{j,M}?$$
2. If such a requirement is reasonable, how can it be satisfied? Modifying the numerical fluxes $\hat{H}^{rk}_{j+1/2}$'s such that
$$u^*_{j,m} \leq u^{n+1}_j = u^n_j - \lambda(\tilde{H}^{rk}_{j+1/2} - \tilde{H}^{rk}_{j-1/2}) \leq u^*_{j,M}, \tag{31}$$
with the new fluxes $\tilde{H}^{rk}_{j+1/2}$'s.

These local bounds

1. $u^*_{j,m}, u^*_{j,M}$ are some local bounds that have to be carefully defined so that they are achievable (at least satisfied by a first order monotone scheme) and not destructive (does not reduce the order of accuracy).
2. If $u^*_{j,m} = \min(u^n_{i-1}, u^n_j), u^*_{j,M} = \max(u^n_{i-1}, u^n_j)$, the scheme will be TVD, thus at most second order accurate.
3. The major challenge is to derive a total variation stability from the bounds.

Reference: Total variation bounded flux limiters for high order finite difference schemes solving one-dimensional scalar conservation laws, MATH COMP 2018, DOI: https://doi.org/10.1090/mcom/3364

The algorithm for the case $f'(u) > 0$

The approach include several simple steps:

1. Calculate preliminary data by using the original high order schemes
$$u_j^{rk} = u_j^n - \lambda(\hat{H}^{rk}_{j+\frac{1}{2}} - \hat{H}^{rk}_{j-\frac{1}{2}}). \tag{32}$$
2. Combine u^{rk} with u^n to create a new vector
$$v(u^n, u^{rk}) = [\cdots, u^n_{j-1}, u^{rk}_j, u^n_j, u^{rk}_{j+1}, u^n_{j+1}, \cdots].$$
It is obvious that $TV_h(v(u^n, u^{rk})) \geq TV_h(u^{rk})$. Thus it is sufficient to require
$$TV_h(v(u^n, u^{n+1})) \ \leq TV(u_0(x))$$
in order for $TV_h(u^{n+1}) \ \leq TV(u_0(x))$.

Characteristic information is used here.

Identify $u^*_{j,m}$, $u^*_{j,M}$

3. Compute $TV_h(v(u^n, u^{rk}))$ and if $TV_h(v(u^n, u^{rk})) \leq TV(u_0)$, flux limiters are not needed. Otherwise let
$$TV_{inc} = TV_h(v(u^n, u^{rk})) - TV(u_0).$$
4. Find all the point values and their locations that contribute to the incremental TV_{inc} in terms of
$$TV_j = |u^n_{j-1} - u^{rk}_j| + |u^{rk}_j - u^n_j| - |u^n_j - u^n_{j-1}| > 0.$$
It is obvious, but important to notice that $\sum_j TV_j > TV_{inc}$.
5. Calculate a proportional parameter $\eta_j = \frac{TV_j}{\sum_j TV_j}$ such that u^{rk}_j is modified according to $\eta_j TV_{inc}$. We use u^*_j to denote the modified value.

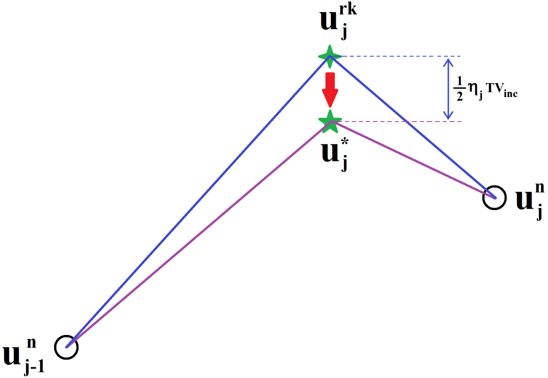

Define the local bounds

$$u^*_{j,m} = \min(u^n_{j-1}, u^*_j, u^n_j), \quad u^*_{j,M} = \max(u^n_{j-1}, u^*_j, u^n_j).$$

Apply the bound preserving flux limiters

6. Pick the lower order monotone flux to be upwinding $h_{j+1/2} = f(u_j^n)$.

7. Modify the high order numerical fluxes $\hat{H}^{rk}_{j+1/2}$'s such that

$$u^*_{j,m} \le u_j^{n+1} = u_j^n - \lambda(\tilde{H}^{rk}_{j+1/2} - \tilde{H}^{rk}_{j-1/2}) \le u^*_{j,M}, \tag{33}$$

with the new fluxes $\tilde{H}^{rk}_{j+1/2} = \theta_{j+1/2}(H^{rk}_{j+1/2} - h_{j+1/2}) + h_{j+1/2}$.

Remark: the flux limiter parameter $\theta_{j+\frac{1}{2}} \in [0, 1]$ is also defined explicitly with a similar process of the BP flux limiter parameter: replacing the global bounds $\{u_m, u_M\}$ by local bounds $\{u^*_{j,m}, u^*_{j,M}\}$.

the TVB scheme for a general $f(u)$

For general $f(u)$, we apply an indirect approach based on the *Lax-Friedrich flux splitting* method: on the time interval $[t^n, t^{n+1}]$, solve an equation

$$v_t + \frac{1}{2}\big(f(v) - \alpha v\big)_x = 0, \quad v(x,0) = u(x,t^n) \tag{34}$$

followed by solving a second equation

$$u_t + \frac{1}{2}\big(f(u) + \alpha u\big)_x = 0, \quad u(x,0) = v(x,t^n) \tag{35}$$

where $\alpha \geq \max_u |f'(u)|$. That is, for one temporal step,

$$u(x,t^n) \Rightarrow v(x,t^n) \Rightarrow u(x,t^{n+1}).$$

$f(u) = u$ and $u_0(x) = \frac{4}{\pi}\arctan(\sin(x))$ (periodic bcs) using the 3rd order linear reconstruction FixR3 and CFL=0.9 at $T = 5$

	N	L^1 error	Order	L^∞ error	Order	$\mathrm{TV}_h(u^n)$
NO flux limiters	40	3.84E-02	–	1.40E-02	–	4.009968
	80	5.60E-03	2.78	2.41E-03	2.54	4.001208
	160	7.25E-04	2.95	3.29E-04	2.87	4.000114
	320	9.17E-05	2.98	4.20E-05	2.97	4.000011
	640	1.15E-05	3.00	5.27E-06	3.00	3.999998
	1280	1.44E-06	3.00	6.59E-07	3.00	4.000000
TVB flux limiter	N	L^1 error	Order	L^∞ error	Order	$\mathrm{TV}_h(u^n)$
	40	3.82E-02	–	1.41E-02	–	4.000000
	80	5.60E-03	2.77	2.41E-03	2.54	4.000000
	160	7.25E-04	2.95	3.29E-04	2.87	4.000000
	320	9.17E-05	2.98	4.20E-05	2.97	4.000000
	640	1.15E-05	3.00	5.27E-06	3.00	3.999997
	1280	1.44E-06	3.00	6.59E-07	3.00	4.000000

$f(u) = \frac{1}{2}u^2$ and $u_0(x) = 1.1 + \frac{4}{\pi}\arctan(\sin(x))$ (periodic bcs) using the 3rd order linear reconstruction FixR3 and CFL=0.9 at $T = 0.5$

	N	L^1 error	Order	L^∞ error	Order	$TV_h(u^n)$
NO flux limiters	40	1.49E-02	–	2.86E-02	–	4.000082
	80	2.71E-03	2.46	8.81E-03	1.70	4.000017
	160	3.92E-04	2.79	1.70E-03	2.37	3.999913
	320	5.15E-05	2.93	2.50E-04	2.77	4.000002
	640	6.55E-06	2.97	3.28E-05	2.93	3.999978
	1280	8.22E-07	3.00	4.14E-06	2.99	3.999996
	N	L^1 error	Order	L^∞ error	Order	$TV_h(u^n)$
TVB flux limiter	40	1.49E-02	–	2.86E-02	–	4.000000
	80	2.71E-03	2.46	8.81E-03	1.70	3.999966
	160	3.92E-04	2.79	1.70E-03	2.37	3.999913
	320	5.15E-05	2.93	2.50E-04	2.77	3.999999
	640	6.55E-06	2.98	3.28E-05	2.93	3.999978
	1280	8.22E-07	3.00	4.14E-06	2.99	3.999996

$f(u) = \frac{1}{2}u^2$ and $u_0(x) = \frac{4}{\pi}\arctan(\sin(x))$ (periodic bcs) using the 3rd order linear reconstruction FixR3 and CFL=0.9 at $T = 0.5$

	N	L^1 error	Order	L^∞ error	Order	$\mathrm{TV}_h(u^n)$
NO flux limiters	20	7.03E-02	–	9.41E-02	–	4.005030
	40	1.52E-02	2.21	3.03E-02	1.64	3.998019
	80	2.31E-03	2.72	5.83E-03	2.38	3.999997
	160	2.97E-04	2.96	1.21E-03	2.27	3.999911
	320	3.63E-05	3.03	1.55E-04	2.97	4.000002
	640	4.42E-06	3.04	1.89E-05	3.04	3.999978
TVB flux limiter	N	L^1 error	Order	L^∞ error	Order	$\mathrm{TV}_h(u^n)$
	20	6.81E-02	–	9.16E-02	–	3.998017
	40	1.52E-02	2.16	3.03E-02	1.60	3.997860
	80	2.31E-03	2.72	5.83E-03	2.38	3.999984
	160	2.97E-04	2.96	1.21E-03	2.27	3.999910
	320	3.63E-05	3.03	1.55E-04	2.97	4.000000
	640	4.42E-06	3.04	1.89E-05	3.04	3.999978

Results for linear advection problem $f(u) = u$

Table: T=0.5, CFL=0.5, $u_0(x) = (1+\sin(x))/2$, FixR=1 with TVB flux limiters

N	L^1 error	order	L^∞ error	order
20	5.30e-03	-	1.31e-03	-
40	6.74e-04	2.98	1.69e-04	2.95
80	8.54e-05	2.98	2.14e-05	2.98
160	1.07e-05	3.00	2.67e-06	3.00
320	1.34e-06	2.99	3.35e-07	3.00

Results

Table: T=0.5, CFL=0.5, $u_0(x) = (1+\sin(x))/2$, ENO3 with TVB flux limiters

N	L^1 error	order	L^∞ error	order
20	5.30e-03	-	1.72e-03	-
40	6.74e-04	2.98	1.89e-04	3.19
80	8.54e-05	2.98	2.37e-05	3.00
160	1.07e-05	3.00	2.83e-06	3.06
320	1.34e-06	2.99	3.69e-07	2.94

Results

Table: T=0.5, CFL=0.5, $u_0(x) = (1+\sin(x))/2$, WENO5 with TVB flux limiters

N	L^1 error	order	L^∞ error	order
20	8.46e-04	-	2.50e-04	-
40	2.52e-05	5.07	8.55e-06	4.87
80	7.47e-07	5.07	2.56e-07	5.06
160	2.28e-08	5.04	7.62e-09	5.07
320	7.10e-10	5.00	2.06e-10	5.21

Results

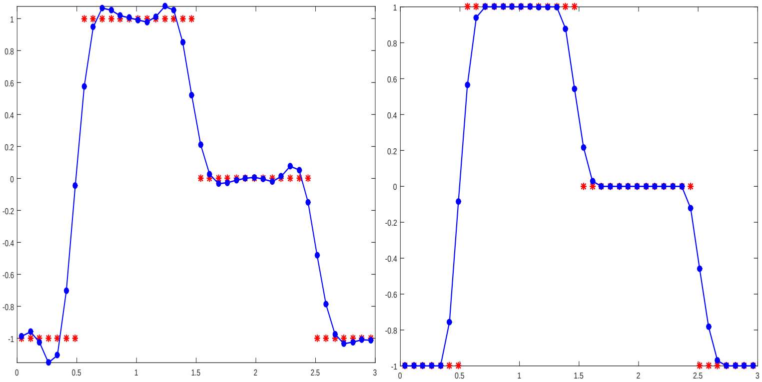

Figure 6: Left: Fix3 without limiters; Right: Fix3 with TVB flux limiters

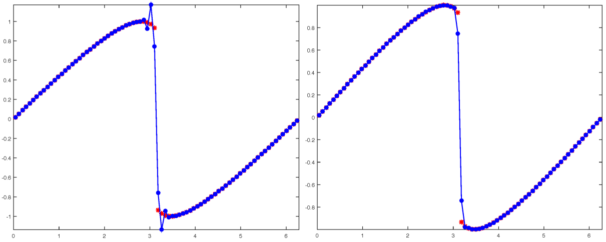

(a) T=1.25, N=80; Sharp TV bounds

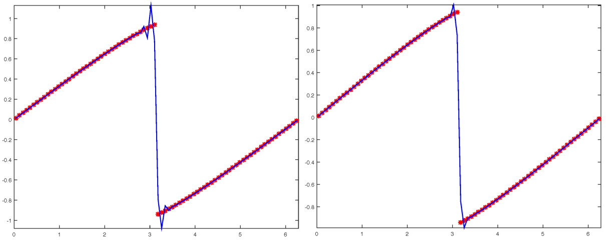

(b) T=2, N=80; Non-Sharp TV bounds

Results after refinement

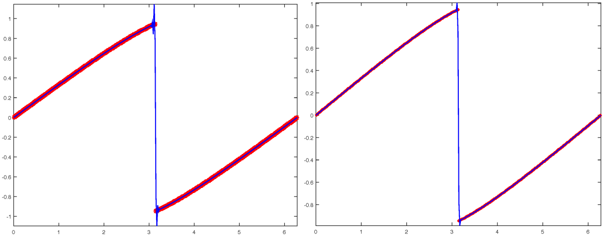

(a) T=2, N=320

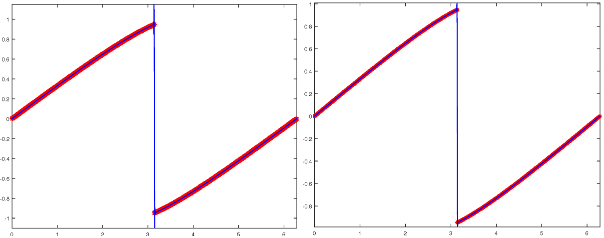

(b) T=2, N=1280

A brief summary

Using the bound preserving flux limiters

1. We design a high order scheme that preserves bounded total variation for scalar conservation laws.
2. The method uses the characteristic information, which makes it hard to generalize to systems.
3. The combined vector approach is also challenging for multi-dimensional problems.
4. The control of oscillation is not complete when the total variation of the solution is well under that of the initial value.

Convexity preserving to identify the local bounds.

Motivation

The purpose is to provide a new approach so that

1. We can find some local bounds that preserves TVB in the original sense.
2. The scheme shall be monotonicity preserving in the monotone region of the solution.
3. The new scheme shall allow Δx^2 level of increase of variation around isolated extrema.
4. It has the potential to be applied to multi-dimension and systems, especially in the latter case where explicit variation bound does not exist.

Basic definition and notations

For one-dimensional problem, we use five consecutive point values to determine the interval on which the function is concave up or down. To distinguish from the traditional definition of convexity, we name such a convexity as **discrete convexity**. For uniform grids,

- The interval $[x_{j-1}, x_j]$ is a concave down interval if
$$u_{j-2}^n - 2u_{j-1}^n + u_j^n \leq 0 \text{ and } u_{j-1}^n - 2u_j^n + u_{j+1}^n \leq 0.$$
- The interval $[x_{j-1}, x_j]$ is a concave up interval if
$$u_{j-2}^n - 2u_{j-1}^n + u_j^n \geq 0 \text{ and } u_{j-1}^n - 2u_j^n + u_{j+1}^n \geq 0.$$

Categorization of the intervals

Let $c_j = u^n_{j-2} - 2u^n_{j-1} + u^n_j$. All the intervals are classified as T1 and T2 type intervals by the discrete convexity.

T1. If $c_j * c_{j+1} > 0$, then $[x_{j-1}, x_j]$ is either a strictly concave up or concave down interval. As we can see that the isolated local maximum or minimum can only be achieved on this type of interval.

T2. If $c_j * c_{j+1} \leq 0$, then interval $[x_{j-1}, x_j]$ does not contain the isolated extrema.

2.cont If the interval is of T2 type, define local bounds as

$$u_{j,m} = \min(u^n_{j-1}, u^n_j), u_{j,M} = \max(u^n_{j-1}, u^n_j). \tag{36}$$

Local bounds for Type 1 interval

As illustrated in Figure 9. $u(t^{n+1}, x_j^*)$ (the blue diamond) represents the same function value as $u(t^n, x_j)$ (the red dot). We assume

1. if the interval $[x_{j-1}, x_j]$ contains an isolated extrema, then $u(t^{n+1}, x_{j-2}^*)$, $u(t^{n+1}, x_{j-1}^*)$ and $u(t^{n+1}, x_j)$ forms the same convexity as $u(t^n, x_{j-2})$, $u(t^n, x_{j-1})$ and $u(t^n, x_j)$.
2. $M1, M2$ can not be exceeded to preserve such discrete convexity constraint.

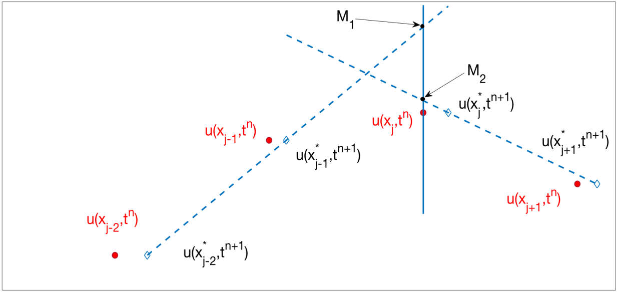

Type 1 interval

If the interval is of T1 type, we first introduce an auxiliary parameter $\beta = u_j^n - \lambda(h_{j+1/2} - h_{j-1/2}) + \text{minmod}(M1 - (u_j^n - \lambda(h_{j+1/2} - h_{j-1/2})), M2 - (u_j^n - \lambda(h_{j+1/'2} - h_{j-1/2})))$ with $h_{j+1/2}$ as the low order monotone flux. We define the local bounds

$$u_{j,m} = \min(u_{j-1}^n, \beta, u_j^n), u_{j,M} = \max(u_{j-1}^n, \beta, u_j^n). \tag{37}$$

We can show

Lemma

The scheme satisfying the upper and lower bounds defined by (36) and (37) is monotonicity preserving.

Numerical results: accuracy

We first test the accuracy of the convexity preserving flux limiters. With a third order Runge-Kutta temporal integration and linear third order spatial reconstruction, we record the accuracy and order of convergence in the following table

N	L^1 error	Order	L^2 error	Order	L^∞ error	Order
20	1.27E-01		1.41E-01		1.99E-01	
40	1.75E-02	2.8521	1.95E-02	2.8516	2.76E-02	2.8489
80	2.23E-03	2.9790	2.47E-03	2.9791	3.50E-03	2.9787
160	2.79E-04	2.9970	3.10E-04	2.9970	4.39E-04	2.9969
320	3.49E-05	2.9995	3.88E-05	2.9995	5.49E-05	2.9994
640	4.37E-06	2.9999	4.85E-06	2.9999	6.86E-06	2.9999
1280	5.46E-07	3.0000	6.07E-07	3.0000	8.58E-07	3.0000
2560	6.83E-08	3.0000	7.58E-08	3.0000	1.07E-07	3.0000

Table 4: The Error and accuracy test with $CFL = 0.6$

We further test the TVB flux limiting combined with the third order linear reconstruction for solving the advection problem with multi wave forms. We can observe the total variation stability evidence form Figure 10.

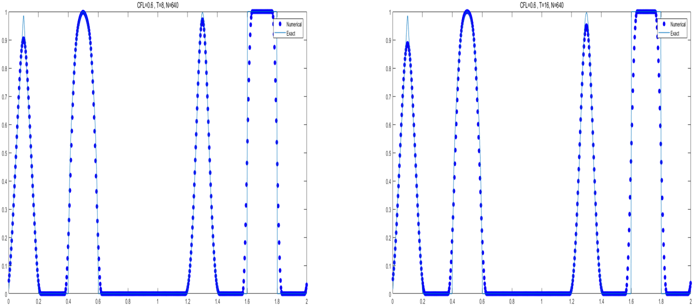

Figure 10: Left: $T = 8$; Right: $T = 16$.

Numerical results: across shock

Our second test case is the Burgers' equation with sine wave as the initial condition. In this computation, we would like to check the performance before and after the shock is developed. The numerical solution is plotted in the following graph.

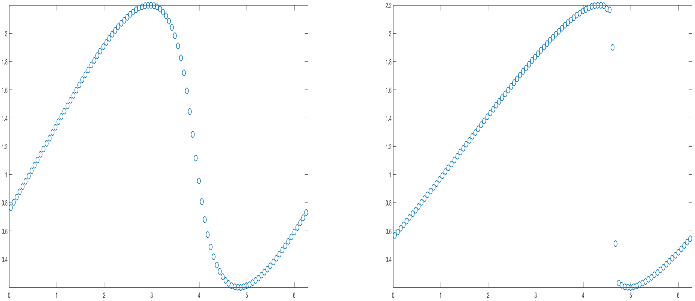

Figure 11: Left: $T = 0.2\pi$, before the formation of shock solution; Right: $T = 0.4\pi$, after the formation of the shock solution.

A brief summary of convexity preserving

As a new approach,

1. It is designed to maintain the non-increasing of number of local extrema and control the magnitude of increase of variation around isolated extrema.
2. Generalization to multi-dimensional scalar problems is ongoing project.
3. It demonstrates favorable results in terms of accuracy and suppression of oscillation around discontinuity.
4. There are a lot of work to do to improve and complete the current approach.

Conclusion and ongoing projects

1. We reviewed the general high order conservative methods in the finite difference setting.
2. We focused on the flux limiting technique to achieve a discrete maximum principle.
3. We generalized the bound preserving method to obtain strict total variation bounded stability for one-dimensional scalar conservation laws.
4. With eyes on multi-dimensional problems and systems, we introduced a convexity preserving constraint to find local bounds so that the bound preserving flux limiting method can be applied to achieve total variation stability.

Thanks for your attention.